

# NSRD-12, Novel Mini-Tubular HEPA Media for Nuclear Facility Ventilation Systems

James Kelly, Nanthakishore Makeswaran, Jamie Maguire,  
Lauren Finkenauer, Jeff Haslam, Mark Mitchell

September 2018



## Disclaimer

This document was prepared as an account of work sponsored by an agency of the United States government. Neither the United States government nor Lawrence Livermore National Security, LLC, nor any of their employees makes any warranty, expressed or implied, or assumes any legal liability or responsibility for the accuracy, completeness, or usefulness of any information, apparatus, product, or process disclosed, or represents that its use would not infringe privately owned rights. Reference herein to any specific commercial product, process, or service by trade name, trademark, manufacturer, or otherwise does not necessarily constitute or imply its endorsement, recommendation, or favoring by the United States government or Lawrence Livermore National Security, LLC. The views and opinions of authors expressed herein do not necessarily state or reflect those of the United States government or Lawrence Livermore National Security, LLC, and shall not be used for advertising or product endorsement purposes.

Lawrence Livermore National Laboratory is operated by Lawrence Livermore National Security, LLC, for the U.S. Department of Energy, National Nuclear Security Administration under Contract DE-AC52-07NA27344.

## Acknowledgements

Financial support was provided by the Nuclear Safety Research and Development Program for the Department of Energy (NSRD-12). Additional support was provided by the Nuclear Science and Security Consortium (NSSC) and DOE/NNSA minority serving institution programs, as well as LLNL's Military Academic Research Associates (MARA) supported by NNSA and DTRA. The authors would also like to acknowledge support from Erick Arevalo, Tony Baylis, Paul Borenstein, Erik Brown, Taylor Bryson, Stephen Cardoza, Samuel Carroll, Robert Deleyos, Dan Flowers, Barry Goldman, Vicki Gravel, Teresa Henrikson, Hazel Holloway, Wayne Jensen, Nicholas Killingsworth, Danny Laycak, Susan Lowder, Dennis Luong, Annemarie Meike, Lemuel Perez, Guillaume Petitpas, Yvonne Pettigrew, Joseph Pickard, Samuel Pogers, Efren Sifuentes, Dwight Squire, Nick Teslich, Alicia Treece, Kathy Tucker, Christine Ward, Howard Wong, Andrew Wood, Clint Worland, and Bethany Goldblum (NSSC/UC Berkeley).



## Table of Contents

<b>1 Abstract .....</b>	<b>5</b>
1.1 Objective .....	5
1.2 Technical Approach .....	5
1.3 Benefits .....	5
1.4 Background .....	5
<b>2 Introduction .....</b>	<b>6</b>
<b>3 Proof-of-Concept .....</b>	<b>8</b>
3.1 Selection of Surrogate Filter Media Stock .....	8
3.2 Fabrication and Testing of Filter Prototypes with Surrogate Media.....	8
<b>4 Development and Testing of Ceramic Nanofiber Mini Tubes.....</b>	<b>10</b>
4.1 Solution Preparation, Mixing, and Storage .....	11
4.2 Electrospinning and Nanofiber Characterization.....	12
4.3 Tube Forming.....	14
4.4 Thermal Treatment and Characterization .....	16
4.5 Filter Integration and Testing .....	17
<b>5 Transition Plan .....</b>	<b>20</b>
<b>6 Conferences, Workshops, and Reports .....</b>	<b>21</b>

## Table of Tables

Table 1. Electrospinning Solution Systems .....	11
---	----

Table 2. Characteristics of the Electrospinning Solutions .....	11
---	----

## Table of Figures

Figure 1. Wide-area deposition of uniform nanofiber membranes by electrospinning and overwrapping tubular ceramic substrates to make filter elements has been previously developed. .....	7
---	---

Figure 2. Pressure drop measurements on filters containing the support media surrogate material (left) or HEPA media surrogate material (right) that demonstrate pressure drop for air flowing through a mini tube filter is lower than for air flowing through a membrane of the surrogate material. This difference is more significant for the HEPA media surrogate, which only meets the target specification of <1 inches of H <sub>2</sub> O at 170 L/min air flow for the mini tube filter. The pressure-drop measurements on the HEPA media surrogate in membrane form agree well with supplier specifications/measurements.....	9
--	---

Figure 3. Process flow diagram to produce novel mini-tubular HEPA filter media, including characterization methods used to support process development. ....	10
--	----

Figure 4. The electrospinning equipment consists of a syringe pump that feeds the electrospinning solution into a hollow needle emitter. A positive bias is applied to the emitter to form a Taylor Cone from which the fiber jet extends. The fiber jet destabilizes and begins to whip within a whipping envelope defined by the electric field. The	
--	--

fibers deposit onto a collector that is maintained at ground or a negative bias. Nanofiber meshes deposited on the collectors are demonstrated in the images. ....	12
Figure 5. Thermogravimetric analysis of nanofibers produced from System 1 and System 2. Both systems lose weight until about 700-800°C. The total weight loss of 66% was observed for nanofibers produced from System 1 and 89% of the weight was lost from nanofibers produced from System 2.....	13
Figure 6. Scanning electron micrographs of nanofiber meshes prepared by electrospinning solutions based on System 1 and System 2. The nanofibers produced from System 1 have a beaded microstructure typically associated with high surface tension and/or low viscosity that leads to partial coalescence when the fiber is still in the liquid state. Bead formation did not occur for System 2, but fibers are sometimes agglomerated into larger threads. Average nanofiber diameter was $82 \pm 14$ nm for System 1 and $141 \pm 16$ nm for System 2, based on a 95% confidence interval.....	14
Figure 7. The fiber mesh deposited on a mandrel from System 1 was brittle and flaked off the mandrel when trying to remove the mesh. The fiber mesh from System 2 was not brittle but did not slide off the mandrel to form tubes. The fiber mesh from System 2 would roll up and eventually tear, but limited lengths could be rolled up and removed from the mandrel to form rings with diameter defined by the mandrel and thickness defined by the length of material rolled off the mandrel. ....	15
Figure 8. Pre-ceramic mini tubes directly removed from a mandrel collector (left) and ceramic mini tubes after thermal treatments. The efficiency of this process was low, and it was difficult to control the tube geometry, so this approach was abandoned. ....	15
Figure 9. Images of pre-ceramic mini-tubular ceramic (MTC) filter media, before thermal treatment, and MTC filter media after thermal treatment. The MTC filter media has reasonable handling strength.....	16
Figure 10. Image of the microstructure for ceramic nanofibers produced from System 2 after thermal treatment. The average fiber diameter is $80 \pm 7$ nm based on a 95% confidence interval. Some fiber de-sintering is observed in the microstructure, possibly suggesting that the nanofibers are not completely free of shrinkage constraints during the thermal treatment.....	17
Figure 11. Pressure-drop measurements through MTC filter prototypes as a function of air flow rate. The pre-ceramic prototype, before thermal treatments, met the target performance unlike the MTC filter prototype. The difference is most likely a result of the different tube sizes and optimization of the tube geometric parameters is recommended.....	18
Figure 12. Aerosol filtration efficiency measurement and extrapolation as a function of depth of filtration for the MTC filter prototype. The filtration efficiency was 49% at a 0.5-inch depth of filtration (DOF). Predictions assuming each 1/2-inch DOF removes an additional 49% of the remaining aerosol indicates a 6-inch depth of filtration is required to achieve HEPA filtration, which is within current geometric constraints on direct-replacement filters.....	19

## 1 Abstract

### 1.1 Objective

The overall goal is to improve safety of DOE nuclear facilities during fire scenarios by developing improved filtration technology, increasing performance while reducing pressure drop. Ceramic filtration technology can provide robust, passive mitigation against radiological releases. The primary objective of this report is to demonstrate that mini-tubular ceramic (MTC) media can reduce pressure drop across a filter compared to flow through a membrane. A secondary objective is to obtain a baseline filtration efficiency measurement. Reducing pressure drop across a filter through MTC design can be combined with nanofiber technology to improve filter performance. Developing MTC media can also solve processing challenges associated with manufacturing ceramic nanofiber membranes and coatings by electrospinning. This work will support developing specifications for industry codes and standards such as ASME AG-1, Subsection FO, Ceramic Filters.

### 1.2 Technical Approach

First, the feasibility of reducing pressure-drop using mini-tubular filtering media was established. Commercial media stock was implemented into prototype filters. The pressure drop across these filters were determined and compared. Second, nanofiber membranes were prepared by an electrospinning process and formed into mini-tubular media. This included refinement of the nanofiber electrospinning process using a variety of ceramic forming precursors and processing parameters. The mini-tubular media was integrated into a prototype to measure the pressure drop across the filter and to obtain and baseline filtration efficiency measurement.

### 1.3 Benefits

The result of this research will help improve safety of DOE nuclear facilities during fire scenarios by developing improved filter technology that provides robust, passive mitigation against radiological releases. Improved filter technology can simplify and reduce safety and support system costs as well as considerably lower life cycle costs, including operational and waste disposal costs. Ceramic filters can operate at much higher temperatures and are inherently safer compared to traditional filters, hence reliance on credited fire suppression systems may likely be eliminated for MTC filters. High-temperature ceramic media such as the kind provided by MTC HEPA filters can result in a sufficiently low pressure drop within a ventilation system and can be substituted into existing filtration systems to reduce costs. Operations of ventilation systems are a key cost driver for DOE nuclear facilities; reducing pressure drop can significantly reduce DOE's operational costs.

### 1.4 Background

This project leveraged past ceramic nanofiber research and development performed by LLNL. Electrospinning ceramic nanofibers has been demonstrated, but implementation into filters has been challenging. This work was intended to demonstrate a strategy for implementing nanofibers into filters by building upon recent advances in polymeric nanofibers used in the biomedical community. Laboratory-scale filter test apparatus is available at LLNL and full-scale filter testing capabilities are available through LLNL collaborators.

## 2 Introduction

Existing HEPA filters can be damaged by fires, water, chemicals, high-pressure, and/or high temperature exposures. Poor performance during emergency scenarios results in significant design, operational, and compliance costs for filter support systems. A ceramic HEPA filter media has the potential to mitigate risks associated with fire, water, or other hazards because many ceramic materials have superior properties compared to other materials that enable them to withstand harsher environments without degradation.

The Defense Nuclear Facilities Safety Board previously highlighted the need for HEPA filter research and development. HEPA filters are a credited element in the defense-in-depth safety strategy for many DOE facilities. Improvements in the fire and water survivability of HEPA filters improve facility safety and reduce dependence on safety support systems. Filters made with high-temperature ceramic materials with sufficiently low pressure-drop across the filter can be substituted into safety class and safety significant filtration systems within ventilation systems. A low pressure-drop across the filter, comparable to current filters, is essential for implementing any new filtering technology without requiring additional system modifications.

This report will demonstrate that mini-tubular media can reduce pressure drop across a filter compared to flow through a membrane and will also cover processes for manufacturing ceramic nanofiber mini-tubular media by using an electrospinning process. The electrospinning process is most commonly used to make polymer nanofiber membranes. It is also possible to make ceramic nanofibers by electrospinning using either sol-gel chemistry or polymer and ceramic precursors that are subsequently converted to ceramic. Both ceramic processes require a thermal treatment after the electrospinning process to obtain the ceramic nanofibers. Shrinkage occurs during the thermal treatment and presents a unique challenge when compared to processing polymer nanofibers.

One method of creating filters involves coating ceramic substrates to make tubular filter elements.<sup>1</sup> Advances in electrospinning have enabled uniform, wide-area deposition of nanofiber membranes that can be used to coat the ceramic substrate. **Fig. 1** demonstrates the integration of polymer nanofibers into this type of filter. One end of the filter element is open, and the other end is closed such that air flow must go through the membrane once fixed into a filter housing. Integrating ceramic nanofibers into a filter prototype by the same methods is more of a challenge. The thermal treatment required to produce ceramic nanofibers by electrospinning can cause substantial shrinkage (e.g., 50-90%). If the fibers are constrained by a substrate, then considerable stress will develop and can tear the nanofiber membrane, which is particularly problematic for deposition over a wide area typical of current HEPA filter media. A tear in the filter media would prevent effective HEPA filtration. Additionally, embrittlement caused by converting polymeric nanofibers with ceramic precursors into ceramic nanofibers precludes developing effective wrapping methods. Tearing can be prevented if the nanofibers can shrink without constraints. Constraints can be eliminated if the nanofibers are formed into a self-supported geometry that enable the nanofibers to shrink freely.

<sup>1</sup> US Patent 9,017,458

## Electrospinning ceramic nanofibers - challenges

Developing wide-area deposition, collection, and overwrapping processes (e.g., polymers)



Shrinkage challenges associated with manufacturing ceramic nanofiber membranes



Shrinkage occurs during thermal treatment and presents a unique challenges for ceramics

**Figure 1. Wide-area deposition of uniform nanofiber membranes by electrospinning and overwrapping tubular ceramic substrates to make filter elements has been previously developed.**

Electrospinning produces a relatively dense coating of nanofibers. As a membrane or film, increasing the thickness can increase the mechanical integrity, but causes a larger pressure-drop in a flow stream through the membrane. This trade-off can be circumvented by using mini-tubular filter media. Generally, filter media with fine microstructures improve filtration. Flow through a tube wall made from nanofibers are expected to have excellent filtration efficiency, but results in a relatively large pressure drop when air flows through the wall. The mini tube approach enables mixed filtration mechanisms to include 1) membrane filtration from flow through the tube wall (high pressure-drop) and 2) contact filtration due to cross flow along the surface of the wall (low pressure-drop). A combination of membrane and contact filtration can result in an intermediate and customizable pressure drop and filtration efficiency regime.

This report builds on recent advances in fabricating self-supported nanofiber mini tubes used in the biomedical research community for vascular substitutes.<sup>2</sup> For example, IME Medical Electrospinning, an electrospinning equipment OEM based out of the Netherlands, now has modules in their product portfolio to produce electrospun tubular constructs.<sup>3</sup> A tubular construct can shrink freely and is therefore suitable for subsequent thermal treatments that convert precursor nanofibers into ceramic.

Specific attributes of this report include 1) the development and testing of prototypes using commercial filtration media as a mini-tubular ceramic filter proof-of-concept, 2) reporting on the development of processes to make mini-tubular ceramic filter media, and 3) development and testing of a mini-tubular ceramic filter prototype.

<sup>2</sup> J. Stitzel et. al., Biomater. 2006 (27) 1088-94.

<sup>3</sup> <http://www.ime-electrospinning.com> (accessed during September 2018).

## 3 Proof-of-Concept

Prototype filters were prepared from commercial filter media stock materials for scoping studies comparing pressure drop from two geometries: mini-tubular and membrane type. The results demonstrate that mini-tubular filter media reduces the pressure drop across the filter in comparison to flow through a membrane. The pressure drop across the prototype filters were measured using a custom-built test apparatus available at LLNL.

### 3.1 Selection of Surrogate Filter Media Stock

Ceramics, glasses, metals, or polymer materials with an open porosity network can be used as a filtering medium. Over 40 manufacturers and suppliers of porous materials available in different forms (tube, pad, paper, and foam stock with different microstructures) were evaluated. The evaluation included publicly available information regarding geometric constraints, minimum and maximum porosity levels, and available pore sizes. These basic metrics were not always readily available. Metrics of direct importance to filter performance (e.g., filtration efficiency and pressure drop) were even less available, most likely because filtration is only a subset of porous materials applications.

Given lack of consistent metrics, best-judgement based on specific goals were used to down-select commercial media stock for the prototype filters. A borosilicate glass microfiber filter paper without a binder phase was selected as a HEPA surrogate material because filter performance metrics were available to compare to our own test results, including pressure drop as a function of air flow rate through a membrane of known diameter and the filtration efficiency. For reference, typical pressure-drop of air flowing through a 47-mm diameter membrane of the HEPA surrogate material was 17 inches of H<sub>2</sub>O at 2 CFM air flow rate. The dioctyl phthalate (DOP) filtration efficiency at 0.3- $\mu$ m sizes determined by ASTM method D-2986 was 99.98% and corresponds to HEPA quality filtration.

The demands on the HEPA support surrogate are less stringent because the primary goal is to provide structural support for HEPA media while minimally affecting the overall pressure-drop. For this purpose, a low-density foam material is a suitable surrogate. A conductive carbon foam was down-selected because it came in low-, medium-, and high-flow grades and is also electrically conductive. The conductivity enables its use as a collector in the electrospinning process, which means it is possible to deposit nanofibers directly onto the carbon substrate.

### 3.2 Fabrication and Testing of Filter Prototypes with Surrogate Media

Carbon media used as a support surrogate were machined into mini tubes. The HEPA filter media used as a HEPA surrogate was cut and wrapped around springs. The seam of the HEPA media wrap on each spring was sealed with super glue. Additional membranes of the media were also prepared. These media types were implemented into filters and tested. Air is pulled through a filter and the test system with vacuum. A valve on the vacuum line is used to throttle the air flow through the system and uses a flow meter for feedback. A manometer is used to measure the pressure drop across the test section where the filter is placed. An upstream aerosol generator and a photometer with upstream and downstream aerosol concentration measurement capability can be used to measure filtration efficiency.

The pressure-drop test results of the prototype filters containing surrogate filter media are given in **Fig. 2**. The pressure drop data for the measurement conditions is approximately linear as a function of air flow rate when plotted on a log-log graph. Linear fits to the data have been extrapolated in **Fig. 2** to lower and higher flow rates than those measured. The support surrogate material meets the pressure-drop specification for this study ( $<1''\text{H}_2\text{O}$  at 170 L/min) for both geometries, but only the mini-tubular geometry meets the pressure-drop specification for the HEPA media surrogate. The difference is attributed to low air-flow resistance through the support surrogate material and high air-flow resistance through the HEPA surrogate material. Relatively high flow resistance is typical of a high-efficiency filter medium. The pressure-drop measurements of the HEPA media surrogate membrane were compared to data from the supplier and the two data sets were in excellent agreement. The pressure-drop for the HEPA surrogate material when tested as a membrane was approximately two orders of magnitude higher than the pressure-drop of the media when using the mini tubular geometry. The pressure-drop test results demonstrate proof-of-concept; the prototype filter having mini-tubular HEPA filter media significantly reduces the pressure drop of air flowing through the filter in comparison to a filter with a membrane of the same filtering material.

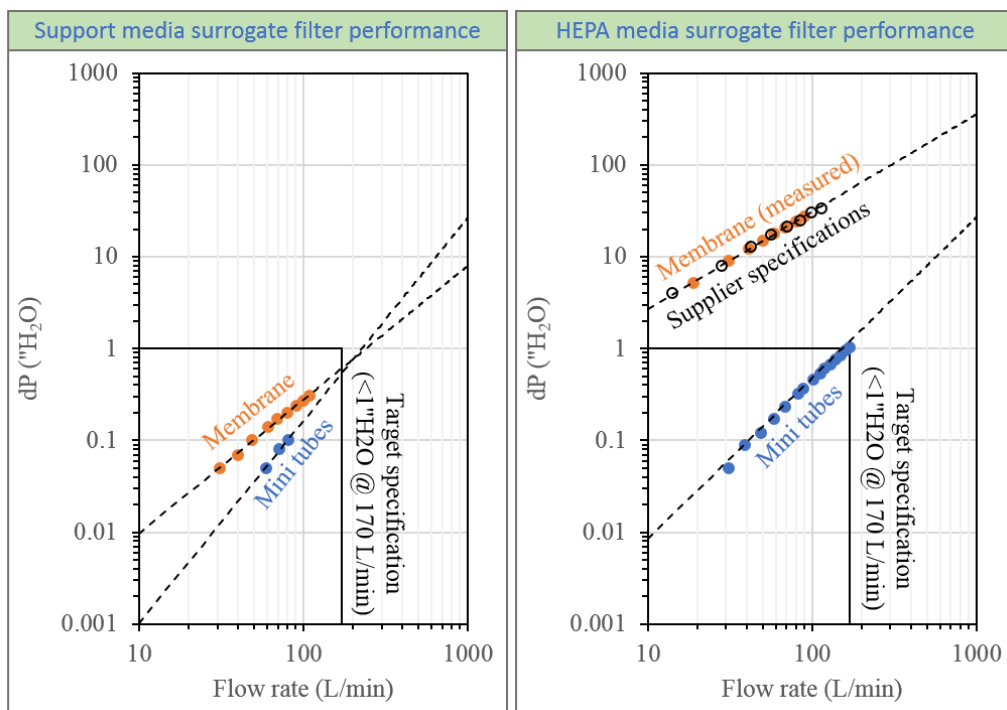


**Figure 2. Pressure drop measurements on filters containing the support media surrogate material (left) or HEPA media surrogate material (right) that demonstrate pressure drop for air flowing through a mini tube filter is lower than for air flowing through a membrane of the surrogate material. This difference is more significant for the HEPA media surrogate, which only meets the target specification of  $<1$  inches of  $\text{H}_2\text{O}$  at 170 L/min air flow for the mini tube filter. The pressure-drop measurements on the HEPA media surrogate in membrane form agree well with supplier specifications/measurements.**

## 4 Development and Testing of Ceramic Nanofiber Mini Tubes

A process flow diagram and the characterization data used to support the process is provided in **Fig. 3**. The process flow diagram is represented by the list down the left side of the diagram and includes solution preparation, solution mixing, solution storage, electrospinning, forming, thermal treatment, and filter integration. Characterization used to support the process includes surface tension measurements, viscosity measurements, electrical conductivity measurements, thermal characterization, structural characterization, and filter performance testing.

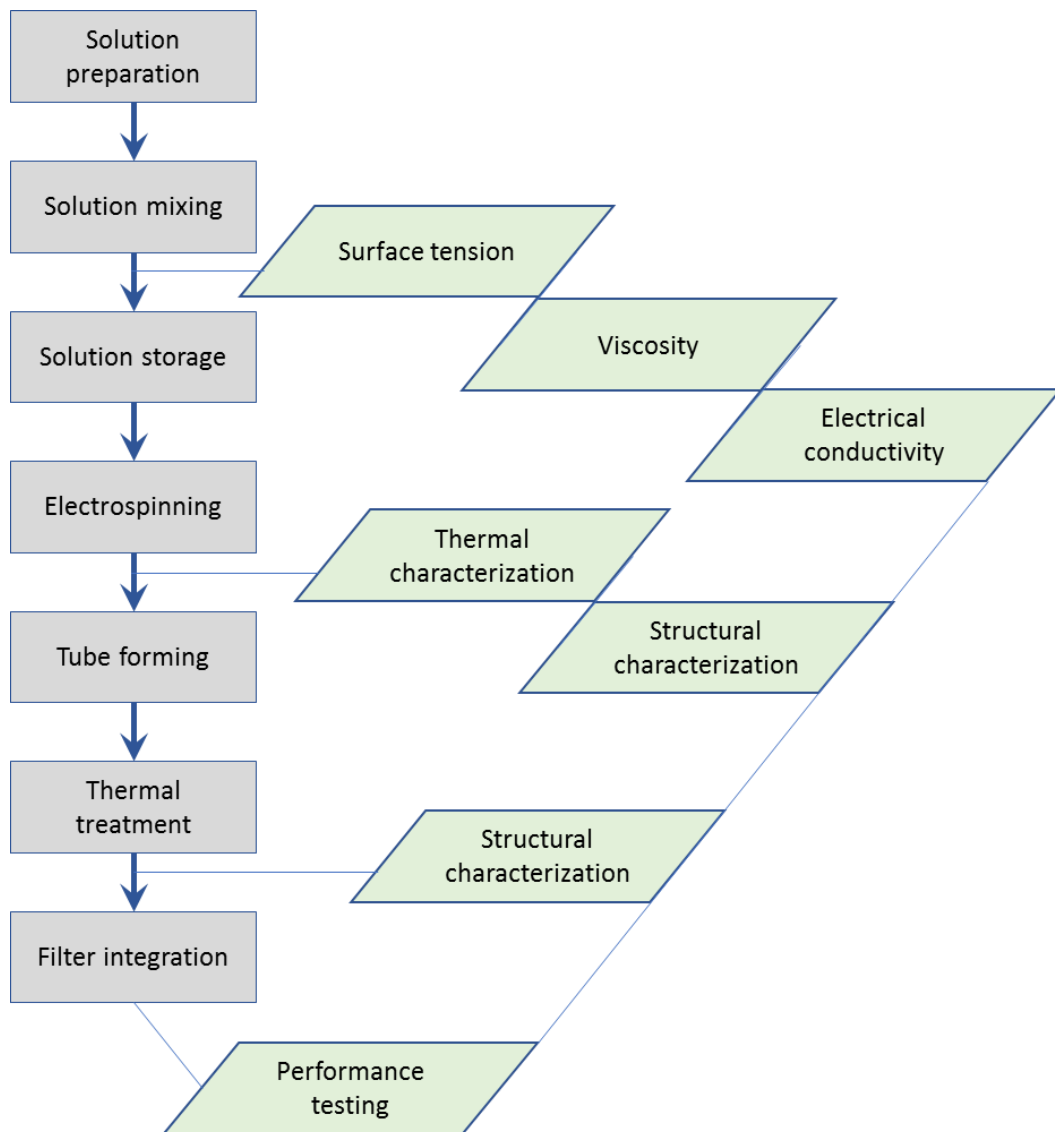


**Figure 3. Process flow diagram to produce novel mini-tubular HEPA filter media, including characterization methods used to support process development.**

#### 4.1 Solution Preparation, Mixing, and Storage

Solutions based on two systems were prepared to leverage prior electrospinning development. The two systems are described in **Table 1**. Both systems utilize water-soluble polymer precursor. System 1 consists of a water solvent, polyvinyl alcohol (PVA) polymer precursor, and Zr-acetate/Y-nitrate ceramic precursors. System 2 consists of a water/ethanol mixed solvent, polyvinyl pyrrolidone (PVP) polymer precursor, and Ga-nitrate ceramic precursor.

**Table 1. Electrospinning Solution Systems**

	System 1	System 2
Solvent(s)	Water	Water/ethanol (50:50 vol.%)
Polymer precursor	Polyvinyl alcohol (PVA)	Polyvinyl pyrrolidone (PVP)
Ceramic precursor(s)	Zr-acetate, Y-nitrate	Ga-nitrate

System 1 uses a PVA polymer precursor. An advantage of using PVA as a polymer precursor is the wide range of PVA grades available to engineer favorable solution characteristics. A disadvantage, however, is that dissolution of PVA into water requires elevated temperatures (e.g., water temperature was controlled at 85-90°C to dissolve the PVA precursor into water before adding the ceramic precursors). System 2 uses PVP polymer precursor that can be dissolved into solution at room temperature before adding ceramic precursor(s). Zr-acetate and Y-nitrate were ceramic precursors added to System 1. These two precursors are used to synthesize Y-stabilized ZrO<sub>2</sub> ceramic nanofibers. Ga-nitrate was the ceramic precursor added to System 2 and is used to synthesize Ga<sub>2</sub>O<sub>3</sub> ceramic nanofibers.

After solutions were prepared, they were mixed overnight at room temperature before characterizing the solutions or storing them for future characterization or use. The solutions were rolled during storage before characterization or use. The solution characteristics are given in **Table 2**. The surface tension of System 1 was 69 mN/m and nearly twice that the surface tension of System 2 (35 mN/m). The lower surface tension of System 2 is attributed to the mixed solvent. The viscosity of the two systems were similar and about 600-700 cP when measured at 1 s<sup>-1</sup> shear rate. The electrical conductivities of the solutions were 63 mS/cm for System 1 and 19 mS/cm for System 2.

**Table 2. Characteristics of the Electrospinning Solutions**

	System 1	System 2
Surface tension (mN/m)	69	35
Viscosity (cP @ 1s <sup>-1</sup> )	650	720
Conductivity (mS/cm)	63	19

## 4.2 Electrospinning and Nanofiber Characterization

The electrospinning equipment used for this work is depicted in **Fig. 4**. The electrospinning equipment consists of a solution feed system, an emitter system, a collector system, and an electrical system. The solution feed system can feed solution to the emitter at rates from 0.1 to 1000 mL/hr. The emitter system is either a single needle, a coaxial needle, or a set of five needles (single or coaxial) and can translate to facilitate uniform deposition onto the collector. The electrical system is used to apply a positive voltage bias (0 to 30 kV) to the emitter system, a negative voltage bias (0 to -10 kV) to the collector system, and powers collector rotation and the exhaust system. The collector system consists of a movable platform to control distance between the emitter and collector and fixturing that enables quick exchange of the collector type and size.

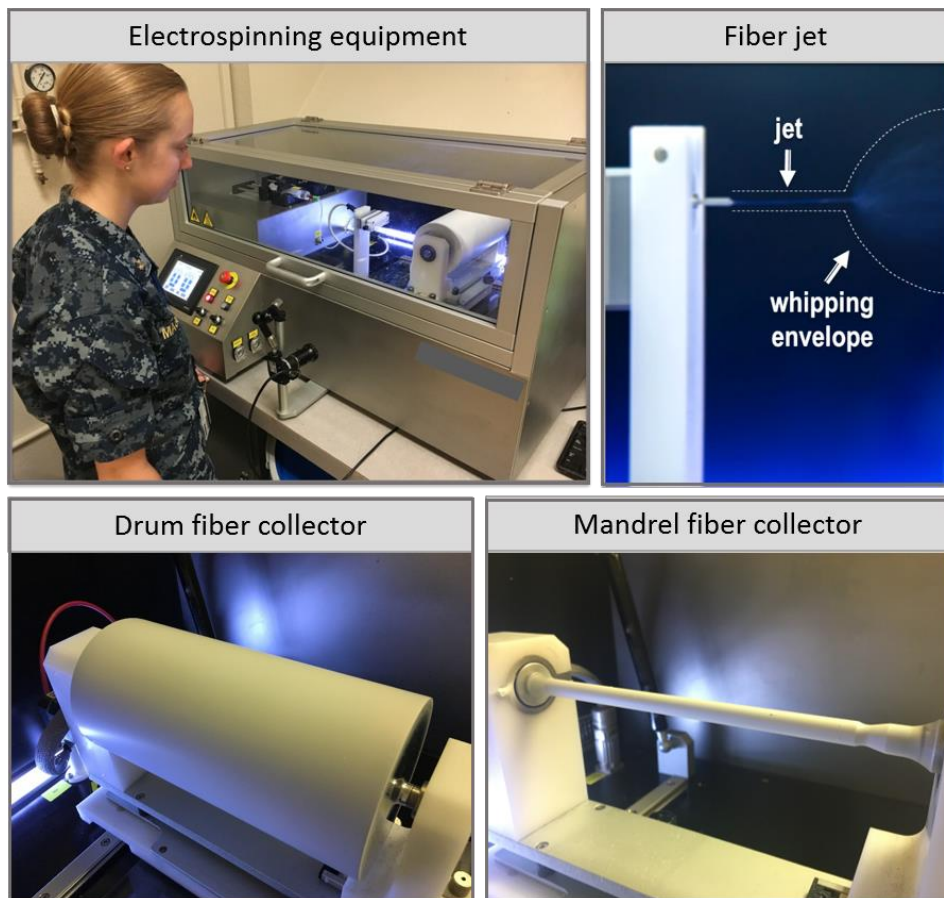


**Figure 4.** The electrospinning equipment consists of a syringe pump that feeds the electrospinning solution into a hollow needle emitter. A positive bias is applied to the emitter to form a Taylor Cone from which the fiber jet extends. The fiber jet destabilizes and begins to whip within a whipping envelope defined by the electric field. The fibers deposit onto a collector that is maintained at ground or a negative bias. Nanofiber meshes deposited on the collectors are demonstrated in the images.

When the electric field is strong enough to overcome surface tension and viscosity, then a Taylor cone forms at the emitter and a fiber jet is ejected if the solution characteristics are suitable. The fiber jet can be stretched and thinned by the electric forces. The fiber jet can eventually destabilize and whip within a whipping envelope, defined by the electric field, before depositing on the fiber collector. If the electrical forces are too high or the solution characteristics are not suitable, then the jet stream can break up into droplets, a process known as electrospraying.

The decomposition behavior of nanofibers produced from System 1 and System 2 are demonstrated by the thermogravimetric results in **Fig. 5**. Weight is lost at different rates as the temperature is increased and corresponds to the decomposition reactions associated with the polymer and ceramic precursor fibers to form ceramic nanofibers. Total weight loss of 66% is observed when forming Y-stabilized  $ZrO_2$  nanofibers from System 1 and 89% is lost when forming  $Ga_2O_3$  nanofibers from System 2. The lower weight loss associated with the  $ZrO_2$  fibers compared to  $Ga_2O_3$  fibers is attributed to higher precursor loading.

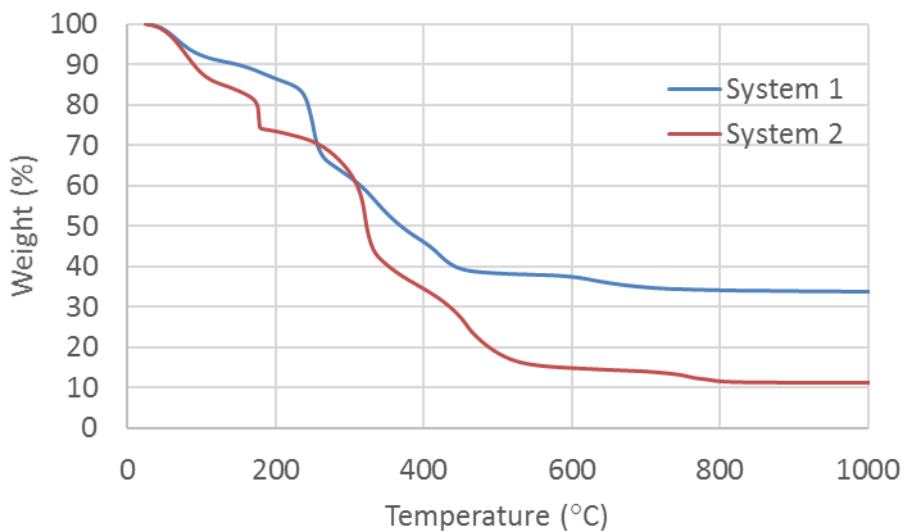


**Figure 5. Thermogravimetric analysis of nanofibers produced from System 1 and System 2. Both systems lose weight until about 700-800°C. The total weight loss of 66% was observed for nanofibers produced from System 1 and 89% of the weight was lost from nanofibers produced from System 2.**

The microstructures of the nanofiber mesh prepared from System 1 and System 2, imaged by scanning electron microscopy (SEM), are demonstrated in **Fig. 6**. Nanofibers from System 1 were beaded, which can be attributed to the relatively high surface tension (69 mN/m) of the electrospinning solution. Nanofibers from System 2 were not beaded because of the relatively low surface tension (35 mN/m) of the electrospinning solution. Pre-ceramic nanofiber diameters of the fibers were on average  $82 \pm 14$  nm based on a 95% confidence interval for nanofibers produced from System 1 and  $141 \pm 16$  nm based on a 95% confidence interval for nanofibers produced from System 2.

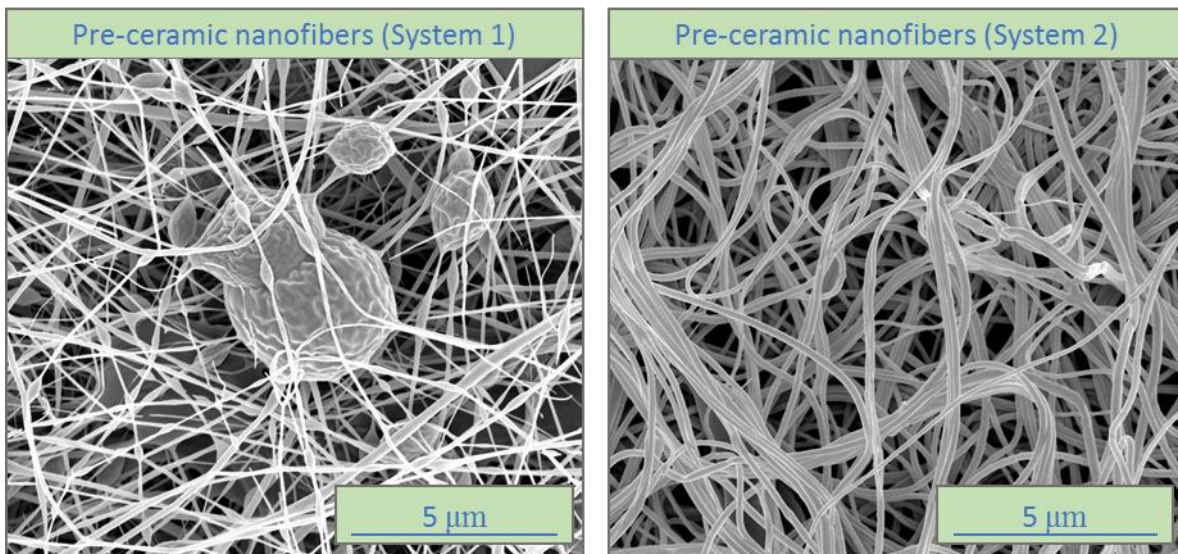


**Figure 6.** Scanning electron micrographs of nanofiber meshes prepared by electrospinning solutions based on System 1 and System 2. The nanofibers produced from System 1 have a beaded microstructure typically associated with high surface tension and/or low viscosity that leads to partial coalescence when the fiber is still in the liquid state. Bead formation did not occur for System 2, but fibers are sometimes agglomerated into larger threads. Average nanofiber diameter was  $82 \pm 14$  nm for System 1 and  $141 \pm 16$  nm for System 2, based on a 95% confidence interval.

### 4.3 Tube Forming

The initial intent was to form tubes by depositing on different-sized mandrels, segmenting the fiber mesh along the length of the mandrel, and removing the mesh as tubes. However, it was not very easy to directly form tubes from either of the electrospinning solutions by removing the mesh from the mandrel this way. The challenges with this approach are demonstrated in **Fig. 7**. The fibers generated from System 1 strongly adhered to the collector and were difficult to remove without flaking apart. A release agent was used to solve release challenge. The brittleness causing flaking is likely attributed to the relatively high loading of ceramic precursor relative to the polymer precursor. System 1 was abandoned because System 2 did not have these problems, but the fibers generated from System 2 were not easily removed from the mandrel either. The mesh would not slide off the mandrel. Instead, the mesh would roll onto itself. If too much of the mesh was rolled up, then it would tear. Suitable lengths could be rolled into rings that could be removed from the mandrel, but the low efficiency of this approach and limited capability to control size compared to a tubular geometry were undesirable and this approach was abandoned. If the size of the mandrel was small (e.g., 2-mm diameter) and long deposition times were used, then it was possible to obtain tubular geometries. Examples of pre-ceramic (prior to thermal treatment) and ceramic mini tubes (after thermal treatment) prepared by this method are given in **Fig. 8**. However, it was difficult to control the dimensions and uniformity of the tubes and low efficiency was still problematic, and so another approach for tube forming had to be explored.

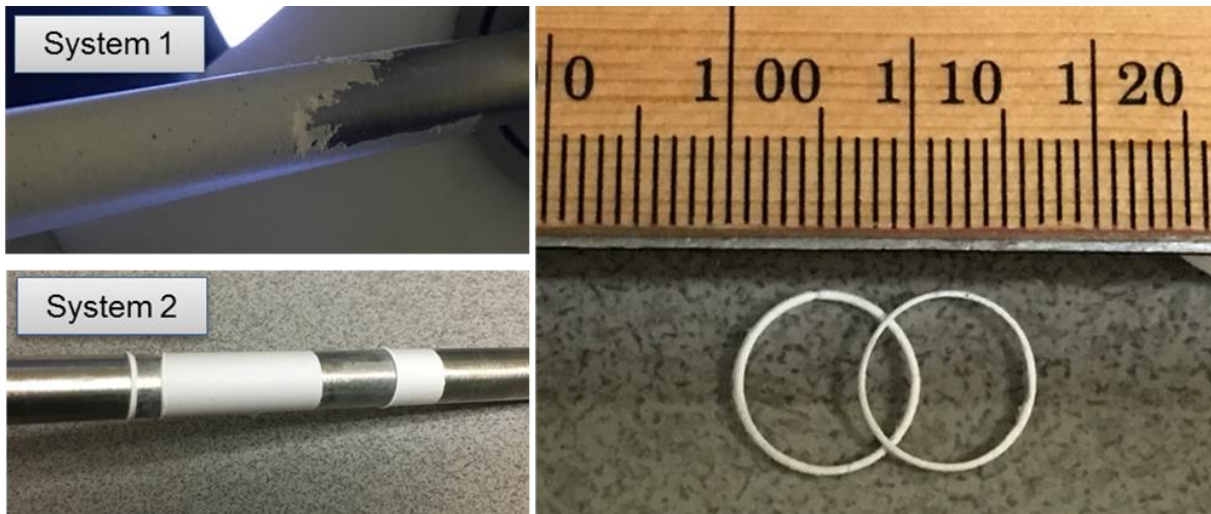


Figure 7. The fiber mesh deposited on a mandrel from System 1 was brittle and flaked off the mandrel when trying to remove the mesh. The fiber mesh from System 2 was not brittle but did not slide off the mandrel to form tubes. The fiber mesh from System 2 would roll up and eventually tear, but limited lengths could be rolled up and removed from the mandrel to form rings with diameter defined by the mandrel and thickness defined by the length of material rolled off the mandrel.

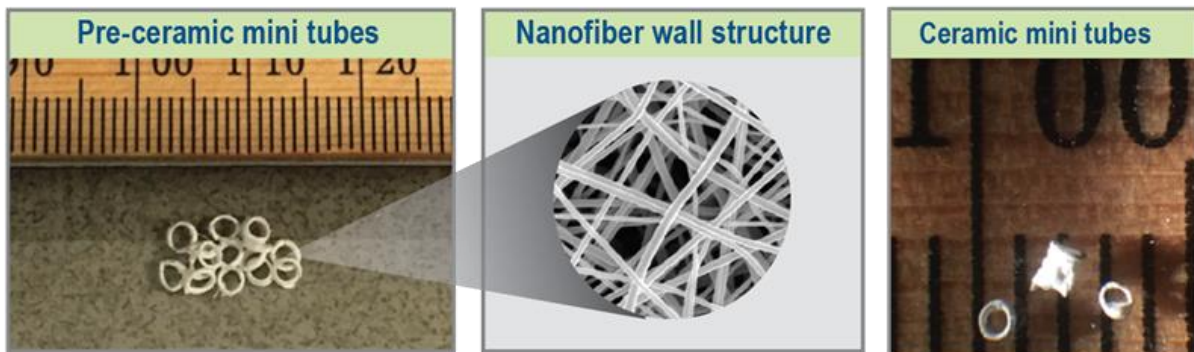


Figure 8. Pre-ceramic mini tubes directly removed from a mandrel collector (left) and ceramic mini tubes after thermal treatments. The efficiency of this process was low, and it was difficult to control the tube geometry, so this approach was abandoned.

Indirect forming of tubes from a sheet of nanofibers was much more efficient than the direct forming trials. A translating emitter was used to deposit the nanofibers onto a drum collector. The nanofiber film was removed from the drum collector after several hours of deposition. The film was cut, wrapped, and the seam was sealed before sliding the tube off the mandrel. This approach allowed us to produce mini tubes at a reasonable production rate.

#### 4.4 Thermal Treatment and Characterization

Thermal treatments were performed by packing the tubes in a crucible and heating in a furnace. The temperature was maintained at a high temperature before cooling back to room temperature. Images of the pre-ceramic mini tubes before the thermal treatment and ceramic mini tubes after the thermal treatment are shown in **Fig. 9**. Comparison between the pre-ceramic MTC filter media, prior to thermal treatment, and the MTC filter media after the thermal treatment demonstrates substantial shrinkage (about 60-70%).



**Figure 9.** Images of pre-ceramic mini-tubular ceramic (MTC) filter media, before thermal treatment, and MTC filter media after thermal treatment. The MTC filter media has reasonable handling strength.

The micrographs in **Fig. 10** show the microstructure of the MTC filter media after thermal treatment. The average fiber diameter after the thermal treatment was  $80 \pm 7$  nm based on a 95% confidence interval, corresponding to about 40% shrinkage during thermal treatment. The fiber diameter shrinkage is less than the overall geometric shrinkage (about 60-70%). Wrinkling of the tubes, as observed in the “tube length” image in **Fig. 9**, is one possible explanation for the higher geometric shrinkage compared to fiber diameter shrinkage. Fiber rearrangement in the non-woven mesh during heat treatment can also contribute to higher geometric shrinkage. Preferred grain orientation within the fibers may also contribute to differential shrinkage in the axial and radial dimensions of the fibers. Possible de-sintering observed in the microstructure suggests that the fibers are constrained, possibly self-constrained where greater shrinkage along the length of the fiber relative to the diameter causes some fibers to break apart. Thicker threads could also provide constraint that prevents uniform shrinkage. Grain sizes within the fibers appear to be on the order of the average fiber diameter, or approximately 80 nm. In some instances, 2-3 grains are observed across the fiber diameter, suggesting grain sizes as small as 20-40 nm.

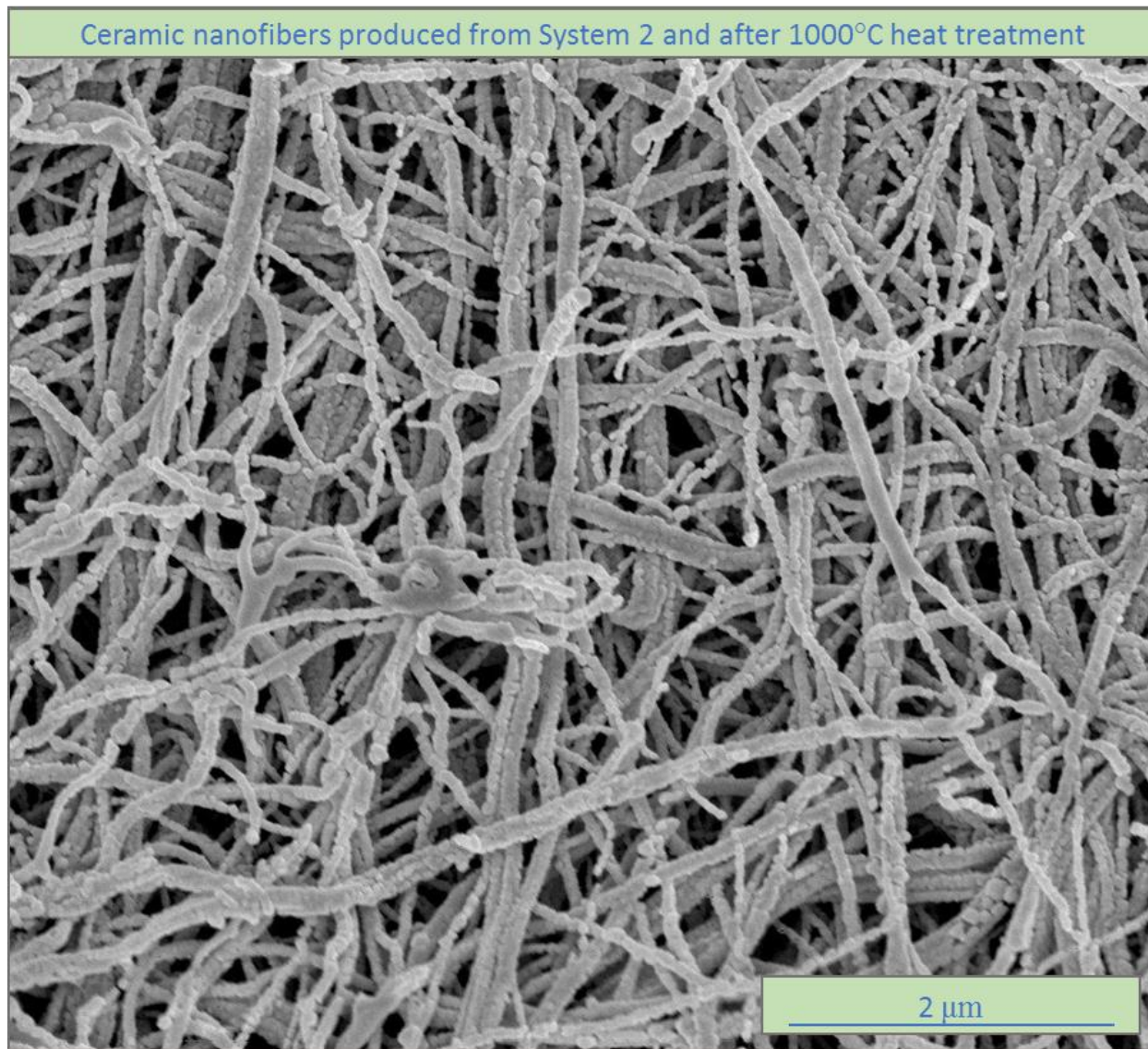


**Figure 10.** Image of the microstructure for ceramic nanofibers produced from System 2 after thermal treatment. The average fiber diameter is  $80 \pm 7$  nm based on a 95% confidence interval. Some fiber de-sintering is observed in the microstructure, possibly suggesting that the nanofibers are not completely free of shrinkage constraints during the thermal treatment.

#### 4.5 Filter Integration and Testing

Filter integration is no different than building the initial prototypes in Section 3.2. Qualitative tests were performed to determine that the mini-tubular ceramic (MTC) filter media had enough strength to integrate into the filter. These qualitative tests demonstrated that no additional precautions were necessary for filter integration. Two MTC filter prototypes were prepared. One of them was prepared with pre-ceramic tubes, prior to thermal treatment, and the other was prepared with ceramic tubes.

The pressure-drop measurements through the two MTC filter prototypes at different flow rates are given in **Fig. 11**. The pre-ceramic MTC filter, before thermal treatment, meets the target performance (<1 inch of water up to 170 L/min) at all air flow rates. The pressure drop of the MTC filter, however, is only <1 inch of water up to 100 L/min air flow. The pressure drop across the MTC filter is up to 2-inches of water at 170 L/min air flow. The difference in pressure-drop performance is most likely a consequence of the tube sizes and indicates feasibility is not ruled out and that optimization of sizes is likely required to achieve specific performance targets. Although not originally intended to be a part of this study, an initial assessment of aerosol filtration efficiency was also performed for the MTC filter and the results are presented in **Fig. 12**. The filtration efficiency was 49% with a 1/2-inch depth of filtration. Predictions assuming each additional 1/2-inch depth of filtration removes an additional 49% of the remaining aerosol indicate that a 6-inch depth of filtration is required for HEPA filtration. This result supports feasibility for a direct replacement of current HEPA filters based on filter geometry constraints.

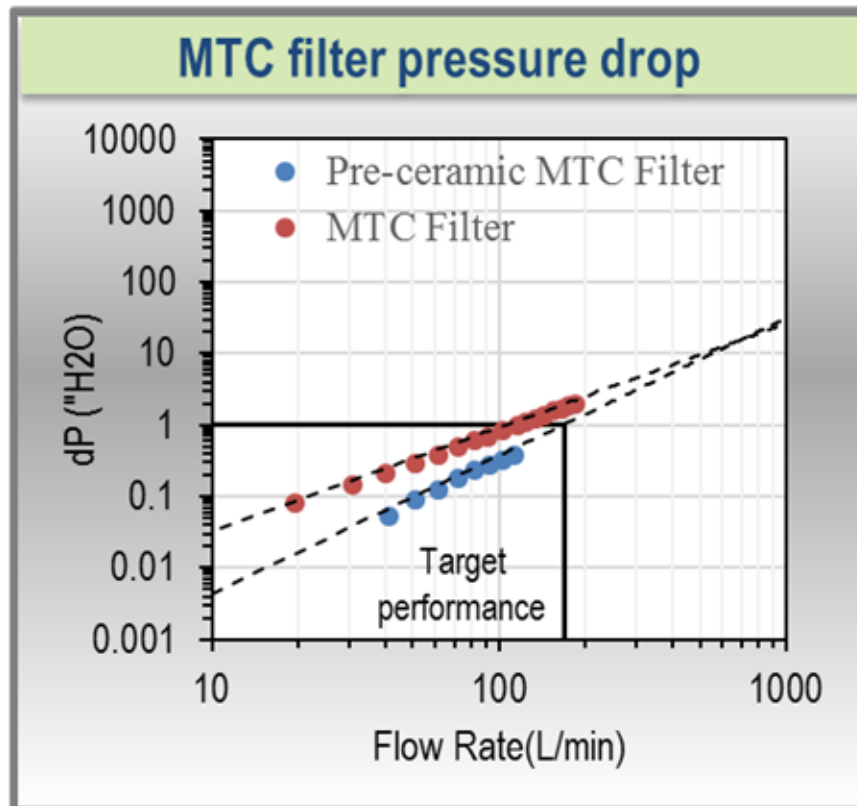


**Figure 11.** Pressure-drop measurements through MTC filter prototypes as a function of air flow rate. The pre-ceramic prototype, before thermal treatments, met the target performance unlike the MTC filter prototype. The difference is most likely a result of the different tube sizes and optimization of the tube geometric parameters is recommended.

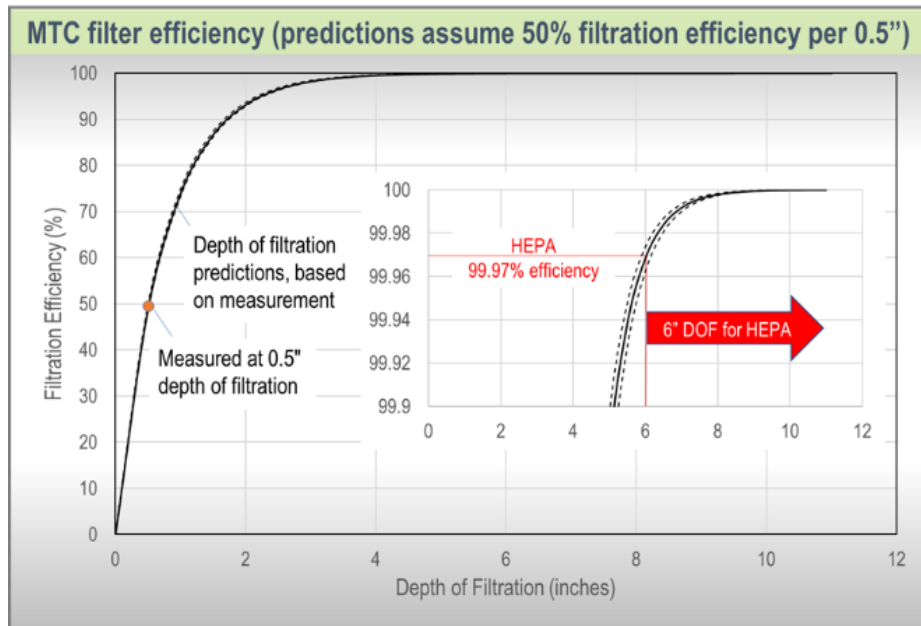


**Figure 12.** Aerosol filtration efficiency measurement and extrapolation as a function of depth of filtration for the MTC filter prototype. The filtration efficiency was 49% at a 0.5-inch depth of filtration (DOF). Predictions assuming each 1/2-inch DOF removes an additional 49% of the remaining aerosol indicates a 6-inch depth of filtration is required to achieve HEPA filtration, which is within current geometric constraints on direct-replacement filters.

---

## 5 Transition Plan

---

Feasibility has been demonstrated. Further understanding of the effect of tube geometry and microstructure, however, is required to enable optimization of pressure-drop across the filter and filtration efficiency to effectively design filters that meet specific performance requirements. Additionally, productivity of the methods used to develop the MTC filter prototype is low and the process needs to be scaled to develop full-scale filtering element prototypes and full-scale filter prototypes that incorporate multiple filtering elements. Methods that improve productivity of the methods will be beneficial for building application-scale prototypes.

## 6 Conferences, Workshops, and Reports

Aspects of the NNSRD-12 project were presented in posters at several external venues, including national and international conferences (most recent to earliest):

- *2018 EFCOG Nuclear Facility Safety Conference*, EFCOG Nuclear & Facility Safety (NFS), Richland, WA
- *2018 International Nuclear Air Cleaning Conference*, International Society for Nuclear Air Treatment Technology (ISNATT), Charleston, SC
- *2017 LLNL External Review Committee*, Livermore, CA
- *2017 Nuclear Science and Security Consortium (NSSC) National Workshop*, Berkeley, CA

Specifically, the materials were presented as follows:

LLNL-POST-755435, *Development and Characterization of MTC Filter Prototypes*, James Kelly *et al.*, at the

- *2018 EFCOG Nuclear Facility Safety Conference*

LLNL-POST-732199, *Next-Generation HEPA Filters for the DOE Complex*, James Kelly *et al.* at the

- *2017 LLNL External Review Committee*
- *2018 International Nuclear Air Cleaning Conference*
- *2018 EFCOG Nuclear Facility Safety Conference*

LLNL-POST-732199, *Design and Development of Electro-Spun Nanoarchitectures of Materials for Extreme Environment Applications*, Nanthakishore Makeswaran at the

- *2017 Nuclear Science and Security Consortium (NSSC) National Workshop*
- *2018 International Nuclear Air Cleaning Conference*,
- *2018 EFCOG Nuclear Facility Safety Conference*.

Other reports prepared as part of the NNSRD-12 project include:

- LLNL-MI-748207, *Novel Mini-Tubular HEPA Media for Nuclear Facility Ventilation Systems (Project Summary & Status)*
- LLNL-MI-738289, *Novel Mini-Tubular HEPA Media for Nuclear Facility Ventilation Systems (Annual Project Summary & Status)*
- LLNL-MI-726348, *Novel Mini-Tubular HEPA Media for Nuclear Facility Ventilation Systems (Project Summary & Status)*